

## COMPUTATIONAL PREDICTION OF A PROPELLER PERFORMANCE IN OPEN WATER CONDITION

A. Fitriadhy<sup>1\*</sup>, N. Amira Adam<sup>2</sup>, CJ Quah<sup>3</sup>

<sup>1</sup>Programme of Maritime Technology, Faculty of Ocean Engineering Technology and Informatics, Universiti Malaysia Terengganu

<sup>2</sup>Postgraduate Student, Programme of Maritime Technology, Faculty of Ocean Engineering Technology and Informatics, Universiti Malaysia Terengganu  
21030 Terengganu, Malaysia

<sup>3</sup>CEO Numit Enterprise, Seri Kembangan, Selangor, Malaysia

Email: naoe.afit@gmail.com amiraadam.nur@gmail.com seiko.q@numit.com.my

**Abstract** -- In the presence of hydrodynamics phenomena occur surrounding propeller evidently affects accuracy's prediction of thrust, torque and its efficiency. A Computational Fluid Dynamics (CFD) simulations approach is proposed to obtain a reliable prediction of the thrust ( $K_T$ ), torque ( $K_Q$ ), and efficiency ( $\eta$ ) coefficients in an open water conditions. The effect of various blade numbers associated with constant propeller revolution (RPM=1320) and pitch ratio ( $P/D=1.0$ ); is performed within the range of advance ratio from  $0.1 \leq J \leq 1.0$ . The results revealed that the increase of blade number from  $Z=3$  to 5 was proportional to the increase of thrust ( $K_T$ ) and torque ( $K_Q$ ) coefficients; meanwhile, it was reduced the maximum efficiency ( $\eta$ ) that possibly lead to downgrading the propeller performance. It should be noted here, the propeller with three blade numbers ( $Z=3$ ) provides the highest efficiency ( $\eta$ ) up to 78.8% at  $J=0.9$ . These CFD simulation results are very useful as a preliminary study of propeller characteristics.

**Keywords:** CFD; Propeller; Blade number; Torque; Thrust

Copyright © 2020 Universitas Mercu Buana. All right reserved.

Received: January 26, 2020

Revised: March 4, 2020

Accepted: March 10, 2020

### INTRODUCTION

The evolution from the fan blades idea has been successfully modified and explored to be a new generation of screw propeller by the ship propulsion engineer many years ago. Along with the advancement of the screw propeller, various shapes, sizes, angles, and the thickness of the propeller have been created to obtain a matched propeller design with the hull's physical and its operating profile [1].

Marine propeller also has a major influence on converting deliver power from the main engine to achieve the required thrust horsepower (THP). The poor propeller quantities resulted in the inadequate propeller performance will lead to negative effects during its operation, such as propeller slip and cavitation problem [2]. To estimate an adequate propeller configuration, a preliminary prediction of propeller performance open water was highly required.

Several researchers have investigated the propeller performance using theoretical and experimental approaches. The theoretical prediction of propeller performance was conducted via circulation or lifting line theory [3, 4, 5]. However, applying the theoretical approach

has been offered disadvantages and impractical to predict the propeller performance due to neglect a few parameters. Meanwhile, the different method was employed using modeling test by Arazgaldi et al. [6], Taheri and Mazaheri [7] and Elghorab et al. [8] at towing tank and cavitation channel. The experimental method produces a lot of advantages that will create an actual flow situation and obtain an accurate prediction of propeller performance. However, this method approach also offered disadvantages in terms of a time-consuming process, an expensive and complex procedure for various test configurations [9]. According to [10, 11, 12], the Computational Fluid Dynamics (CFD) simulation offered several advantages such as allow to simulate using actual and model geometry scale. Reliable prediction results in the extreme condition of the fluid flow and also have a good agreement with experimental data. Therefore, the CFD method has been recommended to be an alternate solution to predict the propeller performance.

This paper presents a CFD simulation approach to analyze the effect of blades number on propeller performance in the open water. The

simulation here is conducted on NUMECA Fine™/Turbo. This software is utilized by grid generation, flow solver, and post-processing capabilities. The package of CFD, including Autogrid5™ to generate fully hexahedral grid generation, 3D Reynolds Averaged Euler and Navier Stokes flow solver and CFView™ as a post-processing module to visualize the results [13]. In this computational simulation, several numbers of blades are considered, and the result of  $K_T$ ,  $K_Q$ , and  $\eta$  has been comprehensively discussed by visualizing the magnitude of scalar torque and static pressure.

## THEORETICAL BACKGROUND

### Governing Equation

The cornerstone of computational fluid dynamics application, there is consists of fundamental mathematical equations such as continuity, momentum, and energy conservation equation. CFD flow solver (ISIS-CFD) on Numeca Fine™/Turbo was based on the incompressible unsteady Reynolds-Averaged Navier-Stokes equation (URANSE) in which the solver applied

$$\frac{\partial}{\partial t}(\rho u_i) + \frac{\partial}{\partial x_i}(\rho u_i u_i) = -\frac{\partial p}{\partial x_i} + \frac{\partial \tau_{ij}}{\partial x_j} + \rho g_i + F_i \quad (2)$$

where  $p$  is the static pressure,  $g_i$  is the gravitational acceleration,  $F_i$  is an external body force in an averaged Cartesian component of the velocity-vector in  $i^{th}$  direction ( $i=1,2,3$ ), and  $\delta_{ij}$  is the Kronecker delta and is equal to unity  $i=j$  and zero when  $i \neq j$ .

### Turbulence Model

During the simulation, a simple one-equation model has relatively applied to compute

$$\frac{\partial \rho \tilde{v}}{\partial t} + \frac{\partial \rho u_j \tilde{v}}{\partial x_j} = \frac{\partial}{\partial x_j} \left[ \left( \mu + \frac{\mu_\tau}{\sigma} \right) \frac{\partial \tilde{v}}{\partial x_j} \right] + c_{b2} \frac{\partial \tilde{v}}{\partial x_j} \frac{\partial \rho \tilde{v}}{\partial x_i} + c_{b1} \rho \tilde{W} \tilde{v} - c_{w1} f_w \rho \left( \frac{\tilde{v}}{y} \right) \quad (3)$$

The eddy viscosity and damping function are defined as Equations (4) and (5), respectively. Where,

$$X = \frac{\tilde{v}}{v} \text{ and the kinematic viscosity } \nu = \mu/\rho.$$

$$\mu_\tau = f_{v1} \rho \tilde{v} \quad (4)$$

$$f_{v1} = \frac{X^3}{X^3 + c_{v1}^3} \quad (5)$$

It should be noted here that the best practice in turbulence model quantities by considering an

the Finite Volume Method (FVM) for representing the inflow and outflow areas, where the fluid flow is well behaved.

### Conservation Equation

CFD simulation consists of fundamental mathematical equations such as continuity, momentum, and energy conservation equation. The mass continuity equation in conservation form is based on the steady and constant density of incompressible flows was presented in Equation (1). Here, the  $\rho$  is the density,  $U_i$  is the averaged Cartesian components of the velocity-vector in  $i^{th}$  direction ( $i=1, 2, 3$ ) [14].

$$\frac{\partial}{\partial x_i}(\rho u_i) = 0 \quad (1)$$

When the fluid element was moving, the net force on the fluid element equals its mass times the acceleration of the element. Therefore, the global Navier-Stokes equation applied the principle of the linear momentum conservation to solve the problem as expressed in Equation (2).

rotating motions of the propeller. The Spalart-Allmaras transports equation model made for eddy viscosity and not required finer grid resolution to capture the velocity field gradients with algebraic models [15, 16, 17, 18]. For external flow application, the kinematic turbulent  $\nu_t$  ( $m^2/s$ ) in this model can be specified and estimate based on the assumptions,  $\nu_t/\nu = 1$  [12]. Here, the transport model for the working variable is shown in Equation (3).

appropriate grid to estimate the cell meshing size,  $y_{wall}$  as written in Equation (6).

$$y_{wall} = 6 \left( \frac{V_{ref}}{\nu} \right)^{\frac{-7}{8}} \left( \frac{L_{ref}}{2} \right)^{\frac{1}{8}} y_1^+ \quad (6)$$

Note that the reference velocity,  $V_{ref}$  can be taken from the body velocity. The reference length,  $L_{ref}$  should be based on the body length since the estimation of the boundary layer thickness is implied in this calculation.

### Hydrodynamics Theory of Propeller

The propeller performance in open water was examined by quantified the thrust ( $K_T$ ), torque ( $K_Q$ ), and efficiency ( $\eta$ ) coefficients to plot against the advance ratio ( $J$ ). The dimensionless quantities are defined as Equations (7)-(10) [19].

$$J = \frac{V_a}{n \cdot D^2} \quad (7)$$

$$K_T = \frac{T}{\rho n^2 D^4} \quad (8)$$

$$K_Q = \frac{Q}{\rho n^2 D^5} \quad (9)$$

$$\eta = \frac{J K_T}{2\pi K_Q} \quad (10)$$

where  $\rho$  is the water density,  $n$ , the number of propeller rotations per second (*rev/seq*),  $D$  the propeller diameter (m) and ( $V_a$ ) represents for water advance velocity (*m/s*).

### SIMULATION CONDITIONS

#### Propeller Particular

The principal dimension of the propeller is clearly shown in Table 1.

Table 1. Principle dimensions of the propeller

Geometrical parameters	Full Scale	Model Scale
Diameter (mm)	3650	119.25
AE/AO	0.695	0.695
P/D	1.013	1.013
Pitch (mm)	3697.45	120.83
Scale	1:30.6	
Propeller Orientation	Right-hand rotation	

#### Simulation Parameter

In the CFD simulation, there are three different numbers of propeller blades considered with constant propeller rotation, 1320 RPM, and P/D = 1.0, as summarized in Table 2.

Table 2. Matrix of computational fluid dynamics solutions

RPM	Number of Blades (Z)		
	Z=3	Z=4	Z=5
1380	√	√	√

#### Computational Domain and Boundary Conditions

The CFD simulation in NUMECA Fine™/Turbo begins with generating an automatic hexahedral structure grid using AutoGrid5™ tools and several steps to complete the meshing process, such as blades raw type configuration, periodicity number, rotational speed, spanwise grid point number, and wall cell width. These steps required to generate domain as presented in Figure 1.

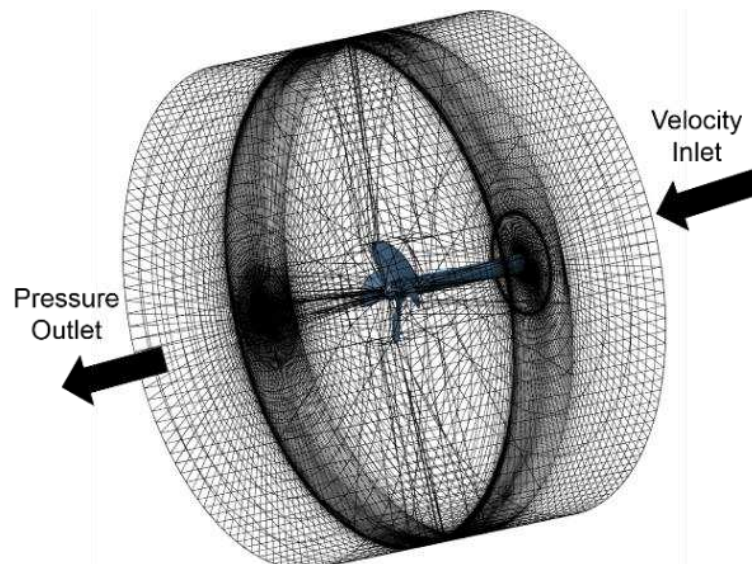


Figure 1. Domain generation of local refinement for velocity inlet and pressure outlet flow direction

The meshing generation should generate surface mesh without any negative cells in a quality report in order to proceed to the simulation

setup. The rounded streamwise O4H grid topology type with 97 grid points in the pitchwise direction has been selected according to the geometry

configuration and grid level [12]. In this case, the turbulence model by the one-equation Spalart-Allmaras model has been applied. The boundary condition was used to set the inlet velocity of the fluid flow and the rotational speed for rotating machinery. This solution serves using the medium grid with 2.8 million total number of cells meshing. The convergence criteria considered here require

a full stabilization of the global quantities, axial thrust, and torque on blades surface [20]. In the final stage of the CFD simulation, a package software in CFView™ was used to visualize the scalar torque and static pressure for all various configurations of the propeller, as displayed in Figure 2.

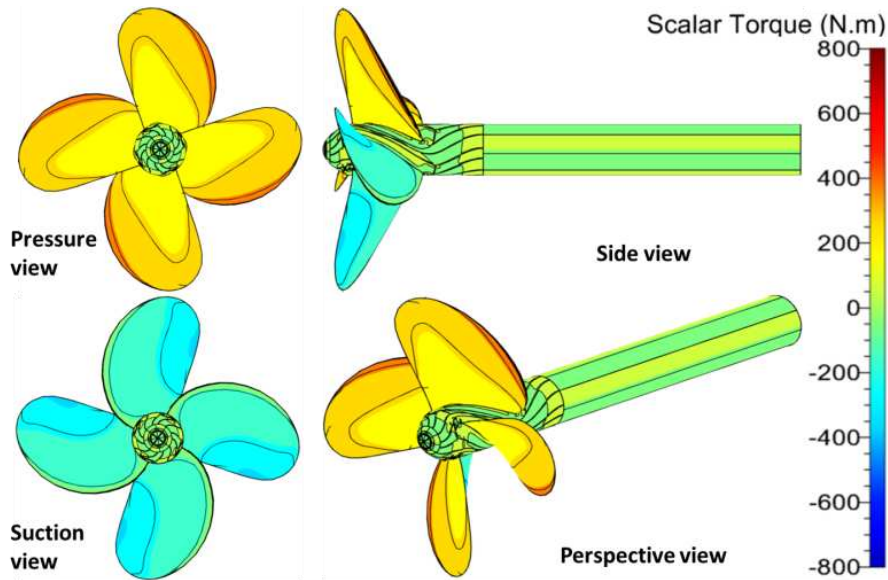


Figure 2. Scalar torque contour visualization for Z=4, J=0.5, RPM=1320

**RESULTS AND DISCUSSION**

The analyses for B-series propeller characteristics in the various blade numbers have been presented and clearly discussed. Computational Fluid Dynamics (CFD) was utilized to quantify the value of torque, thrust, and efficiency coefficients, as displayed in Figure 3. Regardless of blade number, the torque and thrust coefficients have gradually reduced with respect to the increase of advance ratio from J=0.1 up to 1.0. This results analysis was reasonable since the increases in the advance ratio will reduce the drag force on the blade surfaces [21]. As shown in Figure 4, the higher scalar torque value (orange

color) decreased as the advance ratio increased. Furthermore, the efficiency coefficient has relatively increased at a low advanced ratio and decreases at a high advance ratio. With respect to the four blade numbers (Z=4), the efficiency increased within the range of  $0.10 \leq J \leq 0.80$  and drastically decreased at  $J > 0.80$ . This is similar to what was reported by Colley [22] and Yeo et al. [23]. The blue colour region has been expanded at the suction side, which led to a decrease in the propeller efficiency, as shown in Figures 5 (b) and (c).

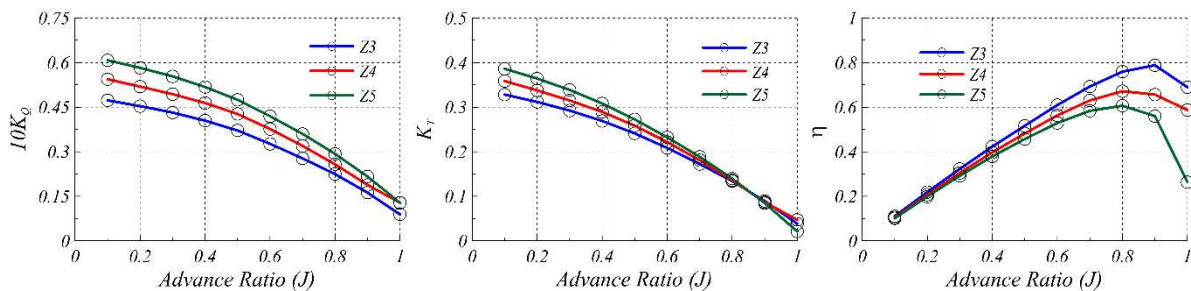


Figure 3. Torque, thrust and efficiency coefficients of the propeller at various blade numbers versus advance ratio

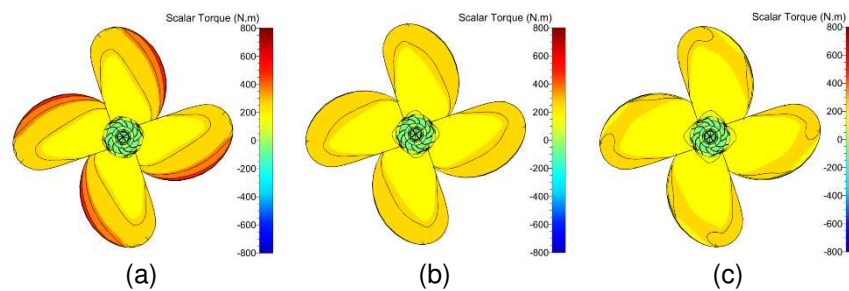


Figure 4. Scalar torque for  $Z=4$  at various advance ratio,  $J= 0.10$  (a),  $J=0.85$  (b) and  $J=1.0$  (c)

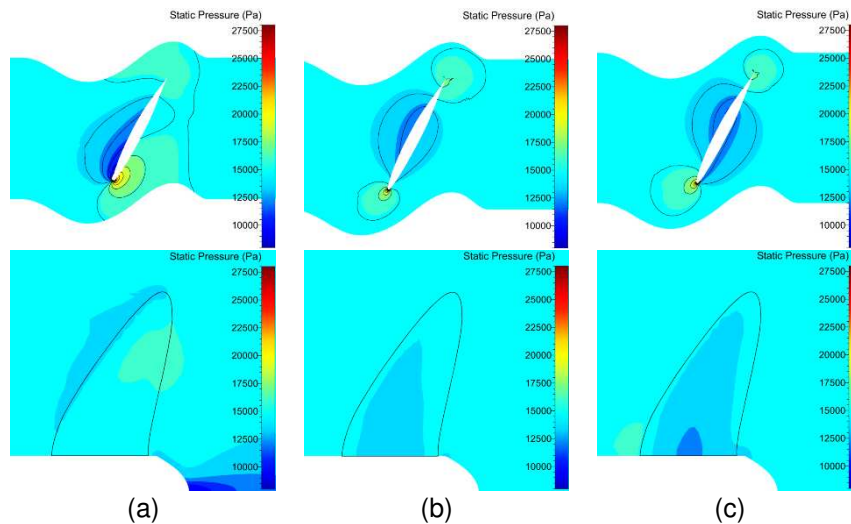


Figure 5 Blade-to-Blade view (top) and meridional view (bottom) of static pressure for  $Z=4$  at  $J= 0.10$  (a),  $J=0.85$  (b) and  $J=1.0$  (c)

By comparing the prediction results obtained from CFD, the propeller with three blade numbers ( $Z=3$ ) produce the highest efficiency with 78.8% at  $J=0.90$ . The subsequent increase of blade number from  $Z=3$  to 4 and  $Z=4$  to 5 was proportional to torque and thrust coefficients; meanwhile, it was reduced the propeller efficiency. Merely, the increase in blade surface area from  $Z=3$  to 5 was proportional to the total drag force (orange contour region) on the blade surface of the propeller, as displayed in Figure 6. The condition is possibly affecting the static pressure at the pressure and suction side of the propeller blade. Similar to what was found by [24], the

increase of thrust coefficient at  $Z=5$  was basically occurred due to the dark blue contour region (low pressure area), as clearly displayed in Figure 7 (c). It can be concluded here that the increase of blade numbers will reduce the static pressure around the propeller blade as supported by [25]. Referring to the CFD simulation results above, it can be concluded that the propeller performance achieved maximum  $\eta$  within the range of  $0.8 \leq J \leq 0.9$  regardless of a number of blades (see Table 3). This inherently indicated that the increase in blade number was degraded the propeller performance.

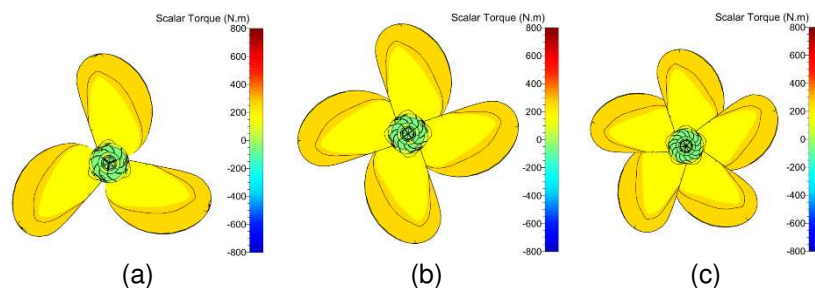


Figure 6. Scalar torque for  $Z=3$ (a),  $Z=4$ (b) and  $Z=5$ (c) at  $J= 0.90$

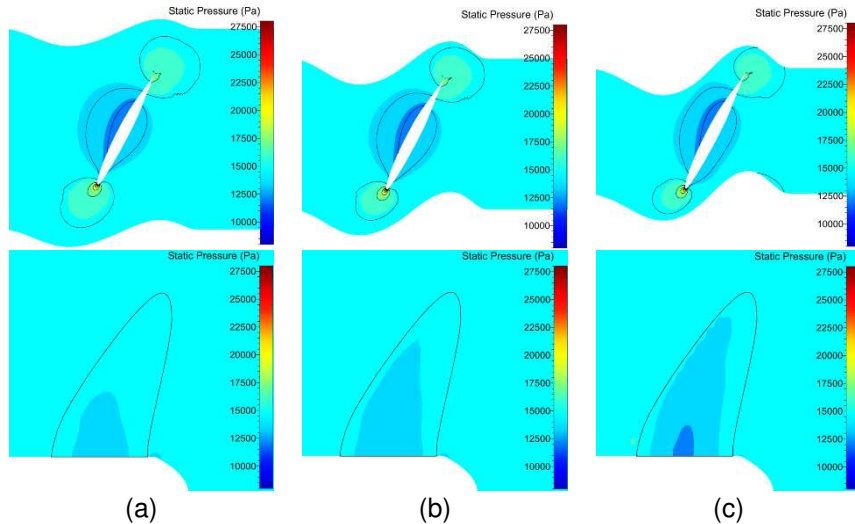


Figure 7. Blade to Blade (top) and meridional (bottom) view of static pressure for Z=3(a), Z=4(b) and Z=5(c) at J= 0.90

Table 3. Torque, thrust and efficiency coefficients of propeller at various blade numbers

J	Z = 3			Z = 4			Z = 5		
	10K <sub>Q</sub>	K <sub>T</sub>	η	10K <sub>Q</sub>	K <sub>T</sub>	η	10K <sub>Q</sub>	K <sub>T</sub>	η
0.10	0.4729	0.3282	0.1105	0.5441	0.3585	0.1049	0.6079	0.3861	0.1011
0.20	0.4537	0.3117	0.2187	0.5192	0.3375	0.2069	0.5824	0.3640	0.1990
0.30	0.4317	0.2924	0.3233	0.4936	0.3151	0.3048	0.5537	0.3388	0.2921
0.40	0.4047	0.2690	0.4231	0.4640	0.2894	0.3971	0.5181	0.3083	0.3788
0.50	0.3715	0.2411	0.5164	0.4271	0.2585	0.4817	0.4747	0.2726	0.4570
0.60	0.3266	0.2084	0.6094	0.3765	0.2219	0.5627	0.4195	0.2324	0.5289
0.70	0.2774	0.1725	0.6926	0.3196	0.1808	0.6301	0.3598	0.1885	0.5836
0.80	0.2249	0.1341	0.7593	0.2578	0.1360	0.6716	0.2931	0.1396	0.6064
0.90	0.1623	0.0893	0.7882	0.1883	0.0863	0.6566	0.2167	0.0847	0.5602
1.00	0.0893	0.0387	0.6894	0.1284	0.0474	0.5873	0.1278	0.0212	0.2637

**CONCLUSION**

The Computational Fluid Dynamics simulation using Numeca Fine™/Turbo was carried out to predict the torque, thrust, and efficiency coefficients of the B-series propeller. The effect of various blade numbers with respect to advance ratios within the range of  $0.1 \leq J \leq 1.0$  has been considered. The situation can be concluded as an increase of the blade numbers results in a subsequent increase of the torque and thrust coefficients. However, this was inversely proportional to the magnitude of its efficiency coefficient. The propeller with Z=3 has gained the highest efficiency of 78.8% as compared to blade numbers of Z=4 and Z=5. In general, the maximum values of the efficiency occurred within the range of  $0.8 \leq J \leq 0.9$  regardless of the various blade numbers.

**ACKNOWLEDGMENT**

The authors wish to greatly thank for P.T. Terafulk Megantara Design for providing the propeller model.

**REFERENCES**

- [1] J. Carlton, *Marine propellers and propulsion*, 4<sup>th</sup> Edition. Butterworth-Heinemann, UK, 2018.
- [2] W. Miller, and J. A. Szantyr, *Practical Design of Marine Propeller*, Gdansk University of Technology: CTO SA, 2010
- [3] B. Epps, J. Ketcham, and C. Chrysostomidis, "Propeller blade stress estimates using lifting line theory," *Proceedings of the 2010 Conference on Grand Challenges in Modeling & Simulation*, Ottawa Ontario, Canada, July 2010, pp. 1-6.
- [4] S. Ekinci, "A practical approach for design of marine propellers with systematic propeller series," *Brodogradnja: Teorija i praksa brodogradnje i pomorske tehnike*, vol. 62, no. 2, pp. 123-129, June 2001
- [5] A. Rahman, M. R. Ullah, and M. M. Karim, "Marine Propeller Design Method based on Lifting Line Theory and Lifting Surface Correction Factors," *Procedia Engineering*, vol. 194, pp. 174-181, 2017. DOI: 10.1016/j.proeng.2017.08.132

- [6] R. Arazgaldi, A. Hajilouy, and B. Farhanieh, "Experimental and numerical investigation of marine propeller cavitation," *Transaction B: Mechanical Engineering*, vol. 16, no. 6, pp. 525-533, December 2009.
- [7] R. Taheri, and K. Mazaheri, "Hydrodynamic Optimization of Marine Propeller Using Gradient and Non-Gradient-based Algorithms," *Acta Polytechnica Hungarica*, vol. 10, no. 3, pp. 221-237, January 2013
- [8] M. A. Elghorab, A. A. E. Aly, A. S. Elwetedy, and M. A. Kotb, "Experimental Study of Open Water Non-Series Marine Propeller Performance," Paper presented at the *Proceedings of World Academy of Science, Engineering and Technology, International Journal of Marine and Environmental Sciences*, vol. 7, no. 6, pp. 1-7, June 2013 DOI: 10.5281/zenodo.1075834
- [9] A. Fitriadhy and N. A. Adam, "Heave and pitch motions performance of a monotriscat ship in head-seas," *International Journal of Automotive and Mechanical Engineering*, vol. 14, no. 2, pp. 4243-4258, June 2017. DOI: 10.1528/ijame.14.2.2017.10.0339
- [10] J. Felicjancik, S. Kowalczyk, K. Felicjancik, K. and K. Kawecki, "Numerical simulations of hydrodynamic open-water characteristics of a ship propeller," *Polish Maritime Research*, vol. 23, no. 4, pp. 16-22, December 2016. DOI: 10.1515/pomr-2016-0067
- [11] H. Sun, F. Jing, Y. Jiang, J. Zou, J. Zhuang, and W. Ma, "Motion prediction of catamaran with a semisubmersible bow in wave," *Polish Maritime Research*, vol. 23, no. , pp. 37-44, April 2016. DOI: 10.1515/pomr-2016-0006.
- [12] T. Turunen, T. Siikonen, J. Lundberg, and R. Bensow, "Open-water computations of a marine propeller using open foam," Paper presented at the *ECFD VI-6th European Congress on Computational Fluid Dynamics*, Barcelona, Spain, 20-25 July 2014, pp. 1123-1134
- [13] N. International, "FINE/Turbo v8. 7. User manual," In *NUMECA International Brussels*, 2009.
- [14] S. Prakash, and D. R. Nath, "A computational method for determination of open water performance of a marine propeller," *International Journal of Computer Applications*, vol. 58, no. 12, October 2012. DOI: 10.5120/9331-3636
- [15] S. Deck, P. Duveau, P. d'Espiney, and P. Guillen, "Development and application of Spalart-Allmaras one equation turbulence model to three-dimensional supersonic complex configurations," *Aerospace Science and Technology*, vol. 6, no. 3, pp. 171-183, March 2002. DOI: 10.1016/S1270-9638(02)01148-3
- [16] M. M. Hejlesen, J. T. Rasmussen, A. Larsen, and J. H. Walther, "Implementation of the Spalart-Allmaras turbulence model in the two-dimensional vortex-in-cell method," Paper presented at the *6th European Congress on Computational Methods in Applied Sciences and Engineering*, Vienna, Austria, 2012.
- [17] Č. Kostić, "Review of the Spalart-Allmaras turbulence model and its modifications to three-dimensional supersonic configurations," *Scientific Technical Review*, vol. 65, no. 1, pp. 43-49, 2015
- [18] E. Lorin, A. Ben Haj Ali, and A. Soulaïmani, "An accurate positivity preserving scheme for the Spalart-Allmaras turbulence model. Application to aerodynamics," Paper presented at the *36th AIAA Fluid Dynamics Conference and Exhibit*, San Fransisco, US, 2006, vol. 3743.
- [19] J. Li, D. Zhao, S. Wang, S. Sun, and L. Ye, "Method for the Calculation of the Underwater Effective Wake Field for Propeller Optimization," *Water*, vol. 11, no. 1, pp. 165, January 2019. DOI: 10.3390/w11010165
- [20] A. Fitriadhy, N. A. Adam, C. Quah, J. Koto, and F. Mahmuddin, "CFD Prediction of B-Series Propeller Performance in Open Water," *CFD Letters*, vol. 12, no. 2, pp. 58-68, 2020.
- [21] M. Husaini, Z. Samad, and M. R. Arshad, "Autonomous underwater vehicle propeller simulation using computational fluid dynamic," In *Computational Fluid Dynamics Technologies and Applications*, InTech, 2011. pp. 293-314. DOI: 10.5772/16297
- [22] E. Colley, "Analysis of Flow around a Ship Propeller using OpenFOAM," *Thesis*, Curtin University, 2012
- [23] C. K. B. Yeo, R. Sabatly, W. Y. Hau, and C. M. Ong, "Effects of Marine Propeller Performance and Parameters Using CFD Method," *Journal of Applied Sciences*, vol. 14, no. 22, pp. 3083-3088, 2014. DOI: 10.3923/jas.2014.3083.3088
- [24] D. Boucetta and O. Imine, "Numerical Simulation of the Flow around Marine Propeller Series," *Journal of Physical Science and Application*, vol. 6, no. 3, pp. 55-61, 2016. DOI: 10.17265/2159-5348/2016.03.008
- [25] N. M. Nouri and S. Mohammadi, "A multi-objective approach for determining the number of blades on a NACA marine

propeller," *Brodogradnja: Teorija i praksa brodogradnje i pomorske tehnike*, vol. 67, no. 2, pp. 15-32, June 2016. DOI: 10.21278/brod67202